Ocean Dynamics (2011) 61:187–202
DOI 10.1007/s10236-010-0322-2

Fine sediment dynamics in a shallow lake and implication for design of hydraulic works

Thomas Vijverberg · Johan Christian Winterwerp · Stefan Gert Jan Aarninkhof · Hans Drost

Received: 6 October 2009 / Accepted: 20 July 2010 / Published online: 11 August 2010

Abstract Lake Markermeer is a large (680 km^2), shallow body of water in the middle of the Netherlands, with a mean water depth of 3.6 m. One of the major problems in the lake is its decreasing ecological value which is, among other reasons, caused by a gradual increase of suspended sediment concentration and associated increase of light attenuation in the water column. A thorough understanding of fine sediment dynamics in the lake is a prerequisite for solving this problem. This paper addresses the 3D nature of near-bed sediment dynamics in Lake Markermeer, based on data sampled from a 1-month field experiment in autumn 2007. The campaign involved the collection of 71 bed samples across the lake. At each location, dual-frequency echo soundings were carried out to assess the thickness of the silt layer, and sediment concentration throughout the water column was measured with an Optical Backscatter Sensor (OBS). Moreover, 2-week time series of wave height, water level, current velocities, and near-bed sediment concentration were collected at a single location. The time series of sediment concentration were measured with a regular OBS and an Argus Surface Meter IV (ASM). During the measurement period, flow velocities ranged between 2 and 15 cm/s, wave heights up to 1.2 m were observed and turbidity levels varied between 40 mg/l to more than 300 mg/l. The ASM data generally showed uniform concentration profiles. However, profiles with steep concentration gradients near the bed were found for wave heights above 0.5 m. The field experiments further revealed pronounced 3D structures near the bed during discrete storms. The results are generalized for a wider range of conditions and across the full water depth through application of a 1DV point model, using a two-fraction representation of the grain size distribution. The fine and coarse fractions are found to resuspend rapidly for wind speeds above 5 m/s and 10–12 m/s, respectively, forming a uniform concentration profile if these wind conditions persists. High-concentration (~1 g/l) layers near the bed, containing the coarse sediment fraction, only occur at the onset and towards the end of a storm, when wind speed changes rapidly. It is under these conditions that horizontal gradients in layer density or thickness can transport considerable fine sediment. This transport provides an additional mechanism for the infill of, for instance, silt traps and navigation channels.

Keywords Lakes · Cohesive sediments · Field measurements · Argus surface meter · Sediment traps

Responsible Editor: Ashish Mehta

T. Vijverberg · J. C. Winterwerp
Delft University of Technology,
Stevinweg 1,
2628 CN Delft, The Netherlands

S. G. J. Aarninkhof
Hydronamic Engineering Department,
Royal Boskalis Westminster Ltd,
P.O. Box 43, 3350 AA Papendrecht, The Netherlands

J. C. Winterwerp
Deltares,
P.O. Box 177, 2600 MH Delft, The Netherlands

H. Drost
Rijkswaterstaat Waterdienst,
P.O. Box 17, 8200 AA Lelystad, The Netherlands

Present Address:
T. Vijverberg (✉)
Royal Haskoning,
P.O. Box 151, 6500 AD Nijmegen, The Netherlands
e-mail: t.vijverberg@royalhaskoning.com

1 Introduction

Lake Markermeer is a large and shallow body of water in the middle of the Netherlands. Because of its size and variety of functions (Fig. 2), it is a unique aquatic feature in Europe. Over the years, several problems have arisen in the lake that affect its functioning. One of the major problems is its decreasing ecological value caused by the combination of increasing turbidity levels, a decrease in nutrients, and increasing temperatures and wind speeds. Large amounts of fine sediment are suspended in the water column, even during mild weather conditions. Over the recent decades the situation has become worse; long-term data show increasing light attenuation and turbidity levels (Fig. 1, after Van Kessel et al. 2008). Moreover, the long-term data show large fluctuations in suspended matter, which reveals the event-driving nature of the sediment transport processes.

In shallow lakes, hydrodynamics and sediment transport are driven by wind. Local wind waves induce erosion of the bed ("wave stirring") and a turbulent boundary layer near the bed. Resuspended sediment is transported with the flow (Jin and Ji 2004; Jin and Sun 2007). Gradients in flow velocity over the depth cause turbulent mixing of sediment. In the case of large flow velocities, the sediment becomes fully mixed over the water column, resulting in a uniform concentration profile. The threshold flow velocity that yields uniform concentration depends on, among other factors, the type and grain size of the bed sediment.

Owing to a mean water depth of 3.6 m, waves in Lake Markermeer can easily penetrate down to the bed. Moderate wave conditions are associated with flow velocities of about 0.1–0.2 m/s. For those conditions, this lake can be considered as a weakly dynamic system. Near the bed, high sediment concentrations can occur but sediments may not mix completely over the water column. This yields sediment concentration profiles with strong gradients near the bed, which are associated with variations in fluid density (both vertically and horizontally). Such horizontal density gradients tend to drive high-concentration sediment transport near the bed, which is likely to be affected by buoyancy effects (Winterwerp 2001). It is anticipated that these 3D processes are important for sediment dynamics in the lake.

Understanding total sediment dynamics is necessary to assess the effects of mitigation measures to improve the water quality, such as a silt trap (Vijverberg 2008). This measure is meant to trap fine sediment so that it is no longer resuspended by moderate to rough waves. A particular advantage of a silt trap is that the sediment that is gained from the realization of the trap can be used for other purposes, such as the construction of shallow marshes. This makes a silt trap a cost-effective solution.

Prior to construction of a trap, sediment dynamics is usually examined with numerical models. Several field measurement and modeling studies have been carried out in Lake Markermeer (Van Duin 1992; Van Duin et al. 1992), which are all based on the use of depth-averaged models (such as STRESS2D). These models do not account for 3D sediment transport processes such as near-bed density currents due to strong gradients in sediment concentration.

The present work investigates the 3D near-bed fine sediment dynamics in Lake Markermeer. Dedicated field measurements were carried out for this study. The paper starts with a description of the physical processes in the lake followed by the setup of the measurement program and the analysis of collected data. Simulations are carried out with a 1DV Point Model to interpret the data and to reveal new insights into the 3D sediment dynamics of the lake. Finally, the implication for the design of hydraulic works, such as sediment traps, is discussed.

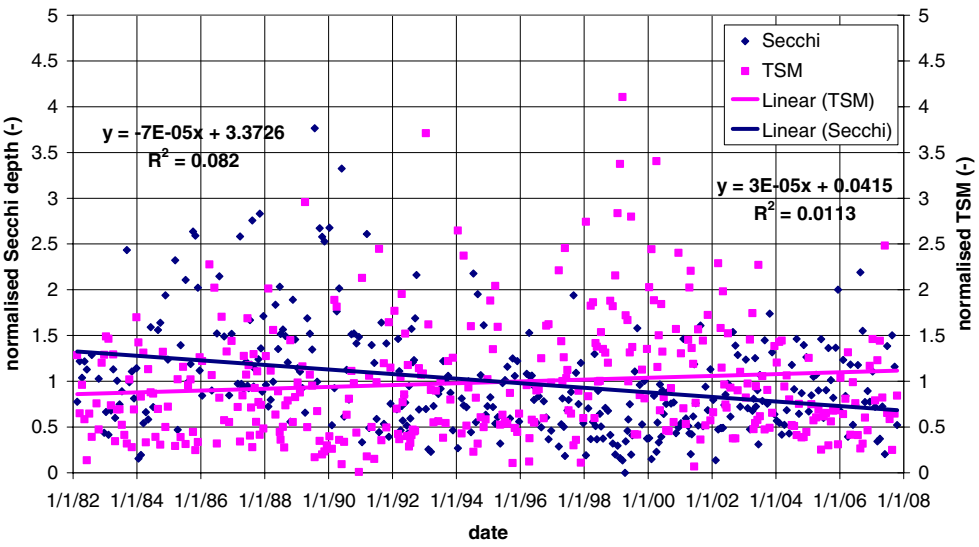

Fig. 1 Secchi depth and total suspended matter over the last 26 years in Lake Markermeer, normalized by the corresponding wind speed (Van Kessel et al. 2008). A long-term trend shows an increase in light attenuation and in suspended matter

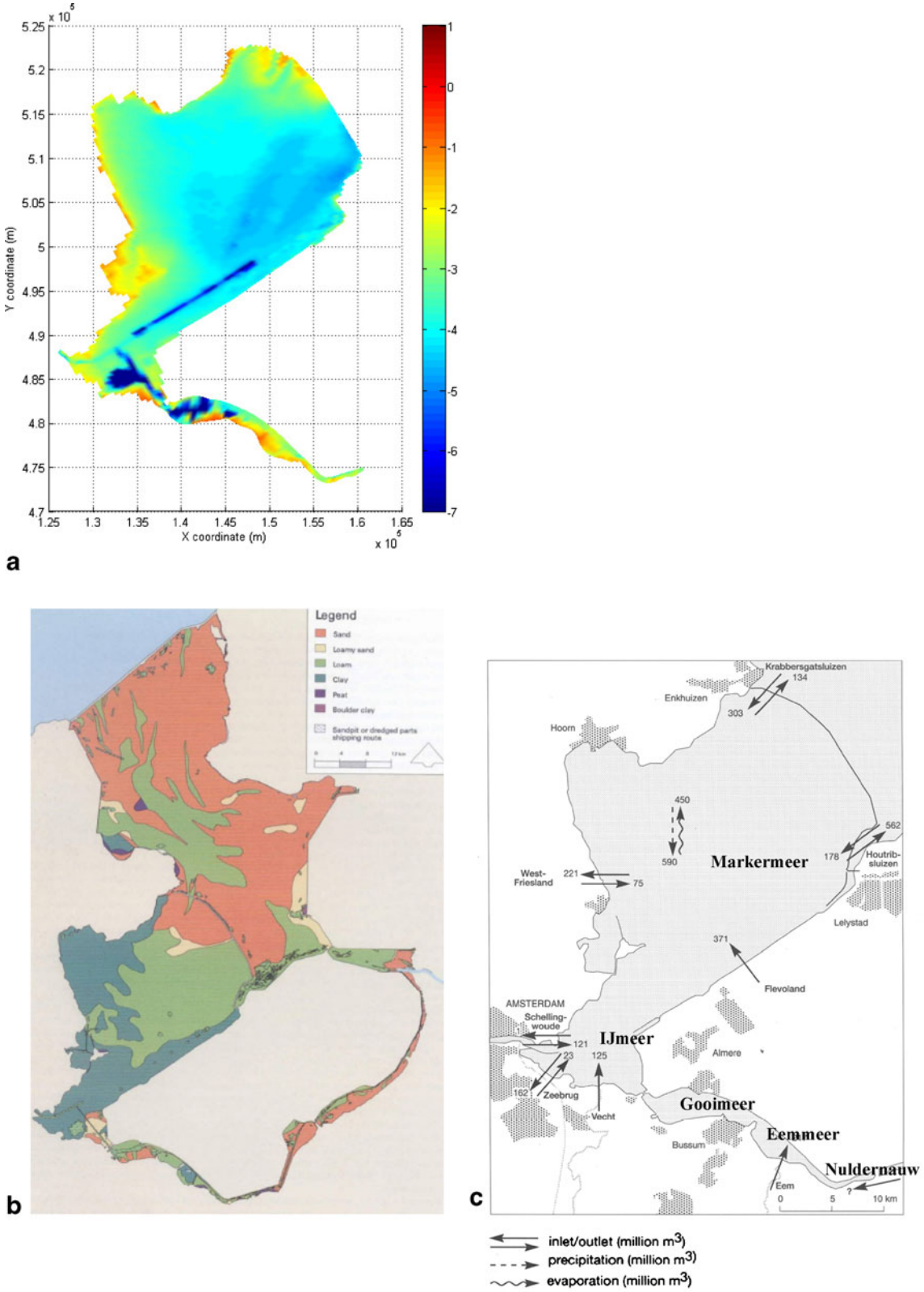

Fig. 2 **a** Bathymetry of Lake Markermeer. In the *south*, deep pits have been dredged; in the *north*, a shallow area occurs. The main part of the lake has a depth between 3 and 4 m. **b** Bed composition (*top layer*) of Lake Markermeer; the clay (dark green) and loam layers (light green) are of marine origin deposited in the pre-Afsluitdijk era (Winkels 1997). **c** Overview of the Lake Markermeer area and water balance for year 1988 (Van Duin 1992)

2 Physical description of Lake Markermeer

The large sea arm, Zuiderzee, in the central part of The Netherlands was isolated from the Wadden Sea, hence from the North Sea, by the construction of a major dike, the "Afsluitdijk" in 1932, forming the freshwater reservoir, Lake IJsselmeer. Within this reservoir, a number of polders were established, and in 1975, the "Houtribdijk" causeway was constructed, which separated the sheltered southern part with clayey bed sediments from the sandy northern part. The southern part became the current Lake Markermeer[1]. This lake has a surface area of 680 km^2 and a water volume of about $2.5 \cdot 10^9$ m^3 with a mean water depth of 3.6 m (Fig. 2a). Almost 50% of the lake has a depth between 3 and 4 m. In the southern part of the lake, pits have been dredged down to 30 m depth.

The upper part of the bed is formed during the Holocene. The bed mainly consists of clay and loam, with some fine to coarse sand in the east (Fig. 2b). The clay layer in the western part of the lake is about 15 m thick, and in the eastern part about 5 to 10 m. In the western part, near the lake shore, some peat layers are also found. In the north (close to the Houtribdike), a shallow sandy area known as the "Enkhuizerzand" occurs. On top of the older sediment layers, fine silt is deposited, covering 60% of the area of the lake, mostly in the southeast. This layer is referred to as the "IJsselmeer deposit" or "silt layer" (Van Duin et al. 1992) and originates partly from the eroded material of older deposits and partly from River IJssel. On top of the deposits, a thin oxidized mud layer is found (only a few millimeters, Fig. 3). This layer contains freshly deposited sediment with a high water content (95%). It is very mobile and is easily resuspended and transported with the flow.

The suspended sediment can be characterized by several mud fractions. Van Duin (1992) and Vlag (1992) provide information on the settling velocities of the fractions obtained from laboratory experiments carried out in 1988 and 1989. Table 1 summarizes the results of those experiments.

The characteristic grain size of the suspended sediment is about 10 μm, as determined from samples after deflocculation. The organic content of the suspended sediment can be high; measured (loss on ignition) values, from a few water samples, are in the range of 18–76% by mass (Vijverberg 2008).

Every year, about $1.1 \cdot 10^9$ m^3 (≈35 m^3/s) of freshwater discharges into the lake through locks, sluices, and small rivers. The total yearly precipitation amounts to about $590 \cdot 10^6$ m^3 (~750 mm/m^2/year), whereas annual evaporation is estimated at $450 \cdot 10^6$ m^3. The average residence time of water in the lake thus amounts to about 6 to 18 months. A summary of the lake's water balance is presented in Fig. 2c. From the hydrodynamic point of view, the lake, together with the neighboring lakes IJmeer, Gooimeer, Eemmeer, and Nuldernauw (Fig. 2c), can be considered as a closed system, with its water movement governed solely by wind effects.

The dominant wind direction in the lake area is southwesterly. Also, during heavy storms, the wind is mostly from that direction. However, there is seasonal spreading in direction. In spring, the winds are usually from the north, in summer from the west, and in autumn and winter (storm season), from the southwest. Waves are wind generated in limited water depth with a maximum fetch of about 25 to 30 km, yielding maximum wave heights of up to 1.5 m with a period of 4–5 s. The flow in the lake is also driven by wind. Wind-induced setup of the water surface balances the wind stress and induces circulation in the lake, which has a strong 3D character. During the southwest winds, the near-surface flow is directed to the northeast in the northern part of the lake. The return flow in the southern, deeper part of the lake is southwest directed. Flow velocities can increase to about 0.20 to 0.30 m/s depending on wind speed and direction. As these are highly variable, complex nonstationary and 3D circulation patterns occur in the lake. These patterns determine the origin and fate of suspended fine sediment.

Information on the bathymetry of the lake, its geological setting (Holocene deposits as well as the Pleistocene layers), and the characteristics of the top layer of the bed can be found in Lenselink and Menke (1995). Van Duin (1992) gives a brief introduction to the sediment characteristics. Water balance, water quality characteristics, and ecological aspects of the lake are described in more detail in Van Duin (1992) as well. Historical wind data of several measurement points around the lake can be downloaded from the website of the Royal Dutch Meteorological Institute (KNMI, www.knmi.nl/samenw/hydra).

3 Measurements in Lake Markermeer

In the autumn of 2007, a measurement campaign was carried out in the lake. It consisted of discrete measurements (multiple locations at specific times) and continuous measurements (time series at one location). The campaign focused on sediment dynamics near the bed. Bed samples and cores were taken together with water column samples. The latter were analyzed for parameters including the grain size of suspended sediment, turbidity, chlorophyll-*a*, phosphorus, pH, conductivity, temperature, and organic content.

At 71 locations across the lake (Fig. 4), bed samples were taken with a Van Veen grab sampler. These samples include the thin oxidized mud layer.

[1] Note that, as in English "mere," in Dutch "meer" means "lake." However, to allow proper geographical reference, we refer to Lake Markermeer rather than Markermeer, or Lake Marken.

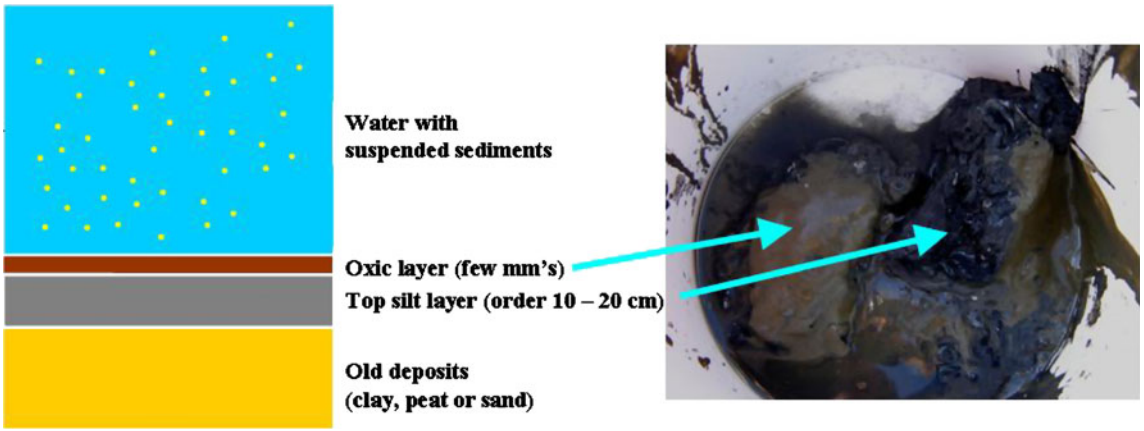

Fig. 3 Photograph of bed sediment sample from Lake Markermeer showing fluffy oxidized and easily mobilized material (*light brown colored sediment*); in the *left panel*, a schematic representation of this bed structure is given

At ten locations cores were taken with a Beeker Sampler for cesium (^{137}Cs) analysis. Two locations (numbers 7 and 8) are shown in Fig. 4. Using a Beeker sampler, cores were taken with 0.6–1.0 m length and a diameter of 0.07 m. The cores were divided into subsamples of 0.20–0.25 m length. For each subsample, the ^{137}Cs content was measured, resulting in a ^{137}Cs profile over the total length of the core. With this profile, the sedimentation history at the locations of the core could be determined (Facchinelli et al. 2001; Sanada et al. 2002; Van Wijngaarden et al. 2002). This technique will be explained in more detail below.

At every measurement location (Fig. 4), dual-frequency echo soundings (type: Knudsen, 320 MP, operating at 33 and 210 kHz) were carried out to measure the thickness of the soft mud layer where it occurred, e.g. Winterwerp and van Kesteren (2004) and McAnally et al. (2007).

Sediment concentrations in the water column were measured with an Optical Backscatter (OBS) sensor (type: Sea Point Turbidity Meter). The sensor was calibrated using nine water samples (250 ml) taken simultaneously with the OBS measurements at a water depth of 2 m. The samples were taken across the lake, spanning a range from 20 to 120 nephelometric turbidity unit (NTU). Laboratory analysis revealed a linear relation between NTU and sediment concentration, i.e. $c = \alpha \times \mathrm{NTU} (\alpha = 0.921, R^2 = 0.917)$, where c is the suspended sediment concentration (sediment mass per unit volume of sample). The high value of α is characteristic of very fine sediment, as in the lake. It was assumed that this calibration relation was valid for all OBS measurements over the lake area. Suspended sediment in the water samples was also analyzed for the grain size distribution using a Malvern particle sizer. The organic content was determined by placing filtered samples in an oven for 1 h at a temperature of 550°C, and then measuring the loss of weight of the sample.

Continuous measurements were carried out at and near the measuring tower FL42 (Fig. 4). At the tower, wave

Table 1 Settling velocities for several mud fractions in Lake Markermeer (Vlag 1992)

	Particle size (μm)	Settling velocity (mm/s)
Fraction 1	<2	0.0025
Fraction 2	2–6	0.020
Fraction 3	7–18	0.090
Fraction 4	>18	0.420

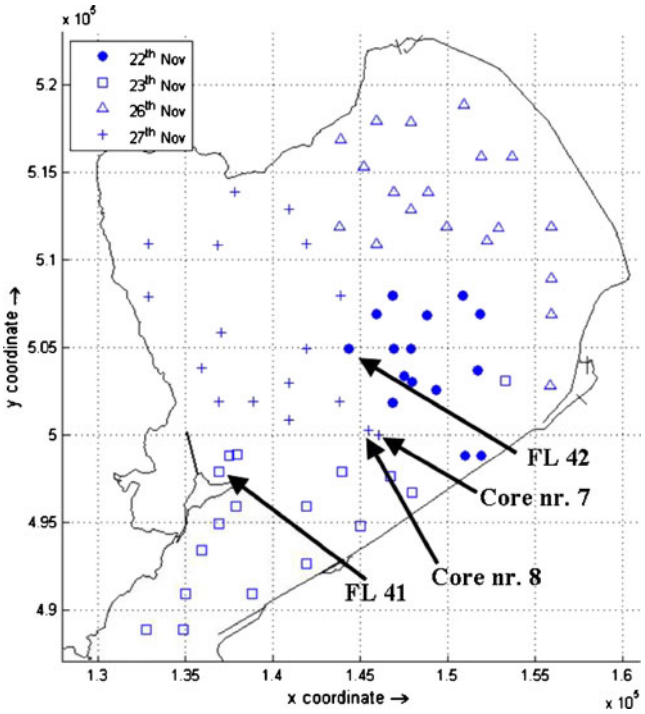

Fig. 4 The 71 measurement locations of the 2007 field campaign. At ten locations, Beeker samples were taken. Core locations *7* and *8* are shown, as well as the measuring towers *FL41* and *FL42*. More information on the exact measurement locations in Vijverberg (2008)

heights were determined with a remote sensing water level gauge (type: LOG_aLevel®, General Acoustics). The measurement interval was 0.25 s. Water levels and wave heights (H_{m0}) were computed every 10 min. Current velocities were also recorded at the tower using an Acoustic Doppler Current Profiler (ADCP, type: Workhorse, RD Instruments, 1,200 kHz). The rate was set at 120 pings/min, and the vertical bin size was 0.25 m. Every 10 min a current velocity profile was taken.

Time series of near-bed sediment concentration were measured 10 m to the southwest of the tower using an Argus Surface Meter IV (ASM). The sediment concentration in the lower 1 m of the water column was measured at an interval of 10 min, and a vertical resolution of 0.01 m (100 sensors), with a range of 5 to 5,000 mg/l. The ASM was mounted on a steel frame, which was placed on the lake bed. On that frame, an OBS (0.50 m above the bed) and an electromagnetic current meter, ECM, (0.25 m above the bed) were also installed to measure turbidity and near-bed velocity, respectively. The measuring period lasted from December 4, 2007, 1200, till December 18, 2007, 1030. The measuring principle of the ASM is identical to the OBS sensor. Calibration was carried out in the laboratory after deployment using bed sediment samples from the lake. A linear relation was found between sensor reflectivity and sediment concentration $c = 1.815\times$ reflection$(R^2 = 0.850)$. This calibration was carried out for six of the 100 ASM sensors. It was assumed that this relation was applicable to all sensors, but the results discussed further in this paper suggest that that assumption might not have been correct. Comparable measurements with the ASM, as well as ^{137}Cs dating of cores, are described in Cundy et al. (2007).

4 Observations

4.1 Flow velocity and waves

Figure 5 presents wave height and flow velocity measured at the FL 42 tower as a function of wind speed. As the tower was placed more or less in the middle of the lake, the fetch for all wind directions was the same, and one would expect a good correlation between wave height and wind speed. This is confirmed in Fig. 5a.

The flow velocity in the middle of the lake, on the other hand, is governed by large scale circulation cells rather than local wind speed. These circulation cells vary with wind direction (e.g., Van Kessel et al. 2008) and have considerable inertia, hence do not respond instantaneously to changes in wind speed and direction. Consequently, the correlation is weaker (Fig. 5b).

Further results on the hydrodynamics are presented in Fig. 8 where time series of turbidity levels are shown, together with time series of wave height and flow velocity.

4.2 Echo sounding

At most locations, the high- and low-frequency echo sounders measured different levels of bed layers, thus revealing the presence of a soft mud layer (Fig. 6a, mud layer thickness of about 0.10 m), as sketched in Fig. 3. The cyclic variation in the echo signal originates from vessel movements due to wave action.

Figure 6b shows the cumulative distribution of the thickness of the soft mud layer based on 57 measurements out of 71 in total; measurements at 14 locations were rejected on the basis of visual inspection of the data. The median mud layer thickness is about 0.1 m, but larger values up to 0.3 m are also measured, most notably in the southeastern part of the lake (close to Lelystad). This coincides with the area where the muddy "IJsselmeer deposit" is found (Van Duin et al. 1992). It is therefore assumed that the layer identified by the dual echo sounder reflects the presence of soft mud across the lake. However, we have no further information on these deposits to confirm this inference.

Note that the thickness of the mud layer at different locations varies with time, as shown in past maps of the thickness of the "IJsselmeer deposit" (Lenselink and Menke 1995). This indicates considerable mobility of this layer, as consolidation alone cannot explain the observed variations in mud layer thickness.

4.3 Cesium

Cesium Cs^{137} measurements can give information about the sedimentation history in the bed of the lake. A peak level of the Cs^{137} content in a core can be related to the Chernobyl disaster in 1986. So these types of measurements can give a direct indication of the sedimentation rate, whereas other measurements (e.g., fall velocity) only give information about the sediment characteristics. In addition, a high Cs^{137} content can mean the presence of fine material in the bed because Cs^{137} binds easier to finer particles, due to the larger surface–volume ratio (van Wijngaarden et al. 2002).

Figure 7 shows typical results of Cs^{137} measurements at locations 7 and 8 (Fig. 4). Cores taken within historical deep pits (e.g. number 7) show significantly higher cesium content (order of 20 Bq/kg DM) than cores taken outside such pits (e.g. number 8, 2 – 4 Bq/kg DM). This indicates that fine sediment does accumulate in the deep pits. Moreover, this further supports the inference that fine sediment is mobile, being transported to quiescent waters.

4.4 OBS

Figure 8 shows a time series of the current velocity and wave height over the ASM turbidity measurement period. Turbidity levels follow the patterns of the wave height

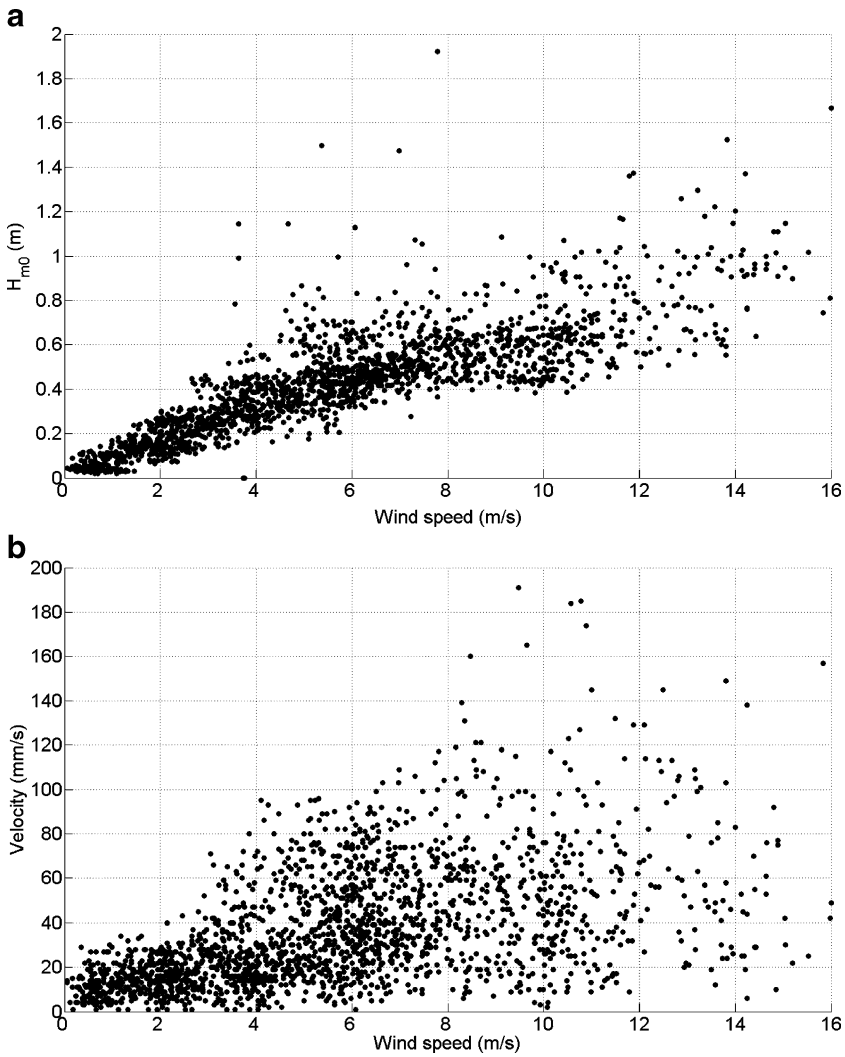

Fig. 5 **a** Scatter plot showing a correlation between wave height and wind speed measured with a remote sensing water level gauge at the measurement tower FL 42. **b** Scatter plot showing a poor, yet positive correlation between flow velocity and wind speed, measured with an ADCP at the measurement tower FL42

closely, and to a lesser extent the current velocity (ADCP). In general, large waves imply high SPM levels and vice versa. This is further illustrated in the scatter plot of Fig. 9 showing a more or less linear correlation between turbidity levels and wind speed, which can be described by $\mathrm{NTU} = 18.1\mathrm{U}_{\mathrm{wind}} + 40 (R^2 = 0.74)$. As wave height and wind speed are also more or less linearly related (e.g., Fig. 5a), we may conclude that an approximately linear relation exists between turbidity and wind speed (or turbidity and wave height). This is a noteworthy observation, as SPM levels usually scale with bed shear stress, which in turn scales with square of wave height.

It is also remarkable that the flow velocity, measured 0.25 m above the bed with the ECM, shows little variation over time, and does not exceed 1.5 mm/s even during storm conditions, whereas the ADCP measures velocities that are an order of magnitude larger and higher in the water column. We believe that the ECM current velocities reflect the flow of mud during stormy periods, but we were not able to verify this.

Figure 10 shows sediment concentration profiles measured with the OBS at four locations. The profiles have been aligned with respect to the water level; the thick black line below the lower measuring point reflects the bed level. In total 66 profiles were obtained at different locations. Figure 10a and b shows very uniform profiles with SPM concentrations between 40 and 60 mg/l. Figure 10c and d shows that highly nonuniform sediment concentration profiles can occur also with near-bed concentrations above 100 mg/l. The near-bed concentration may even be three times higher than in the upper part of the water column (Fig. 10d).

4.5 Argus surface meter

Further information on the vertical SPM profiles in the lower part of the water column was obtained from the continuous ASM measurements. Figure 11 presents vertical profiles at four times indicated in Fig. 8, viz. December 4, 2200 hours; December 5, 2200 hours; December 7, 0650

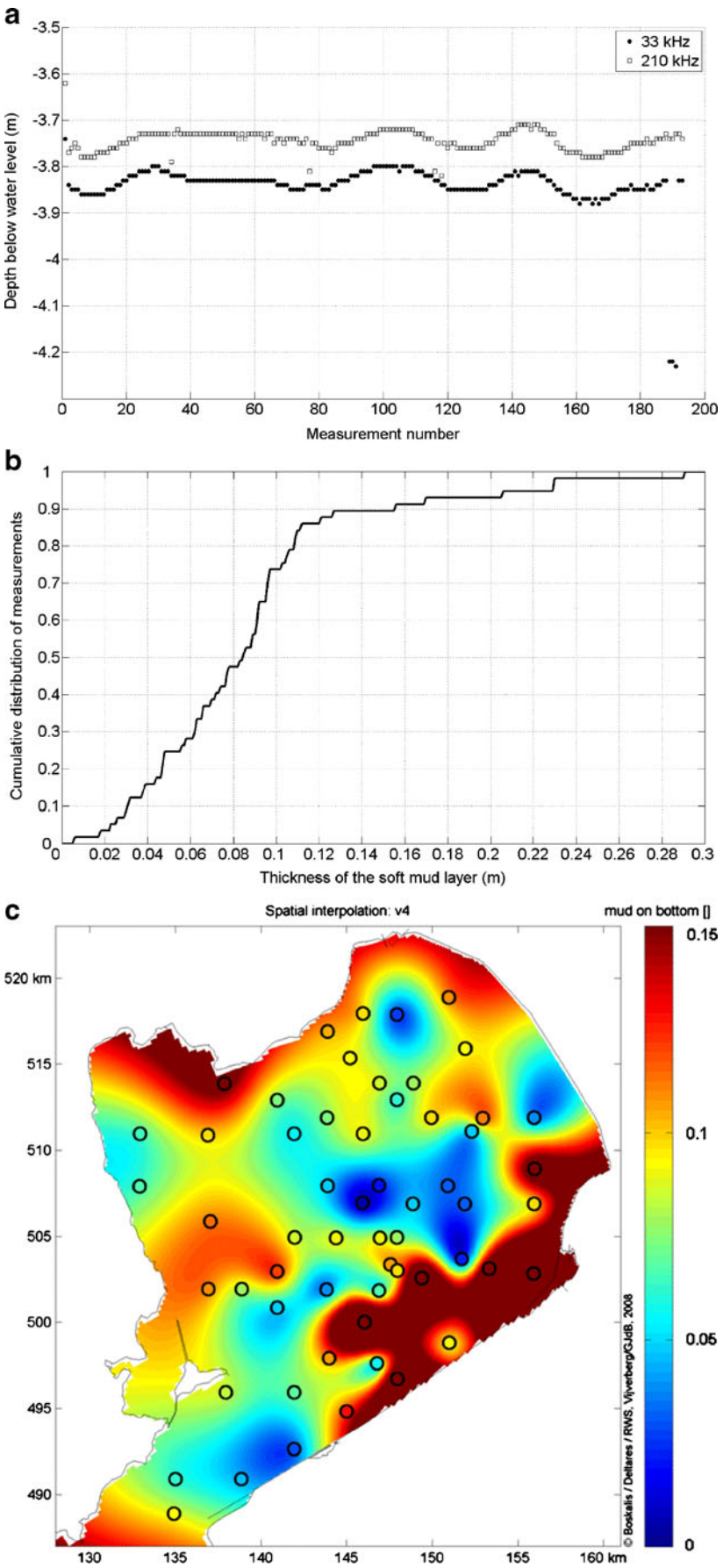

Fig. 6 **a** Typical echo-sounder record on location 12, November 26, 2007, showing mud layer thickness of about 0.1 m (difference between 210 and 33 kHz reflections). Note that the *x*-axis indicates the measurement number. In this case, the measurement period was almost 20 s, so the output frequency was approximately 0.1 s. **b** Cumulative distribution of thickness of soft reduced mud layer in Lake Markermeer with a median value of almost 0.1 m and a maximum thickness of 0.3 m. **c** Thickness of the soft mud layer (in m) over the lake. *Circles* are measurement locations. In the southeastern part of the lake, the mud layer is more than 0.15 m thick

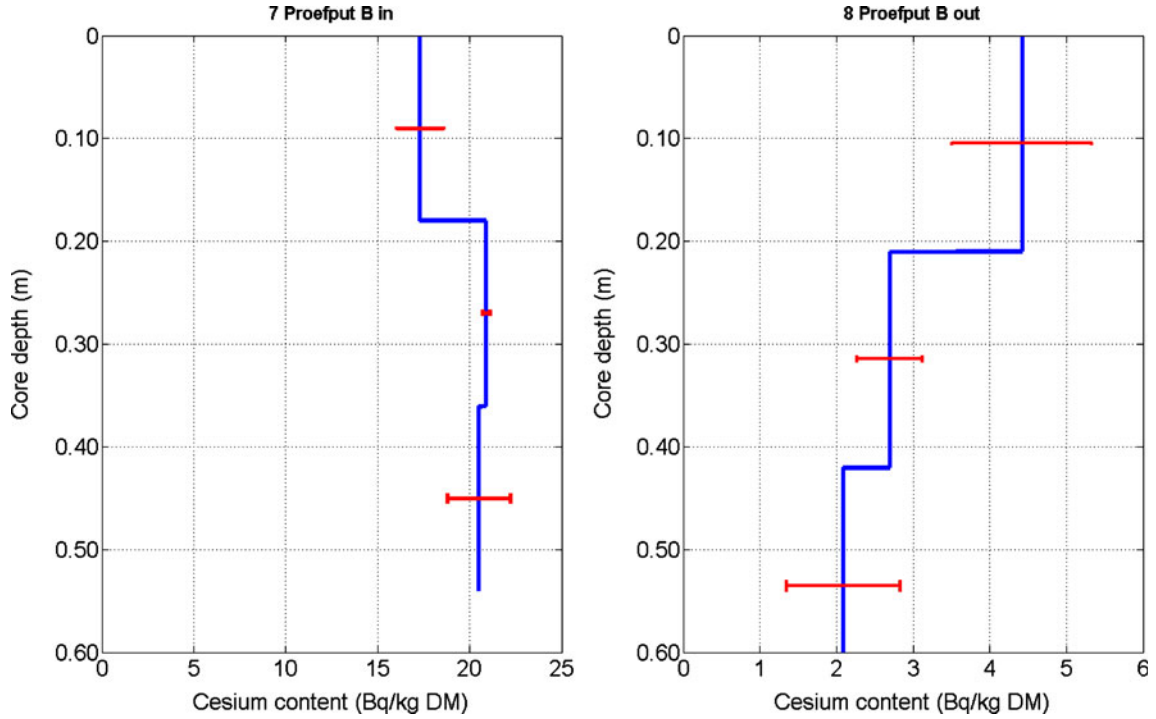

Fig. 7 Cesium profiles measured at two locations as a function of core depth (note different scales). The left profile (no. 7) represents Cs^{137} concentration inside a deep pit, whereas the right profile (no. 8) represents Cs^{137} concentration next to that pit. Inside the pit, the cesium content is much higher, indicating that fine sediments accumulate in deep pits

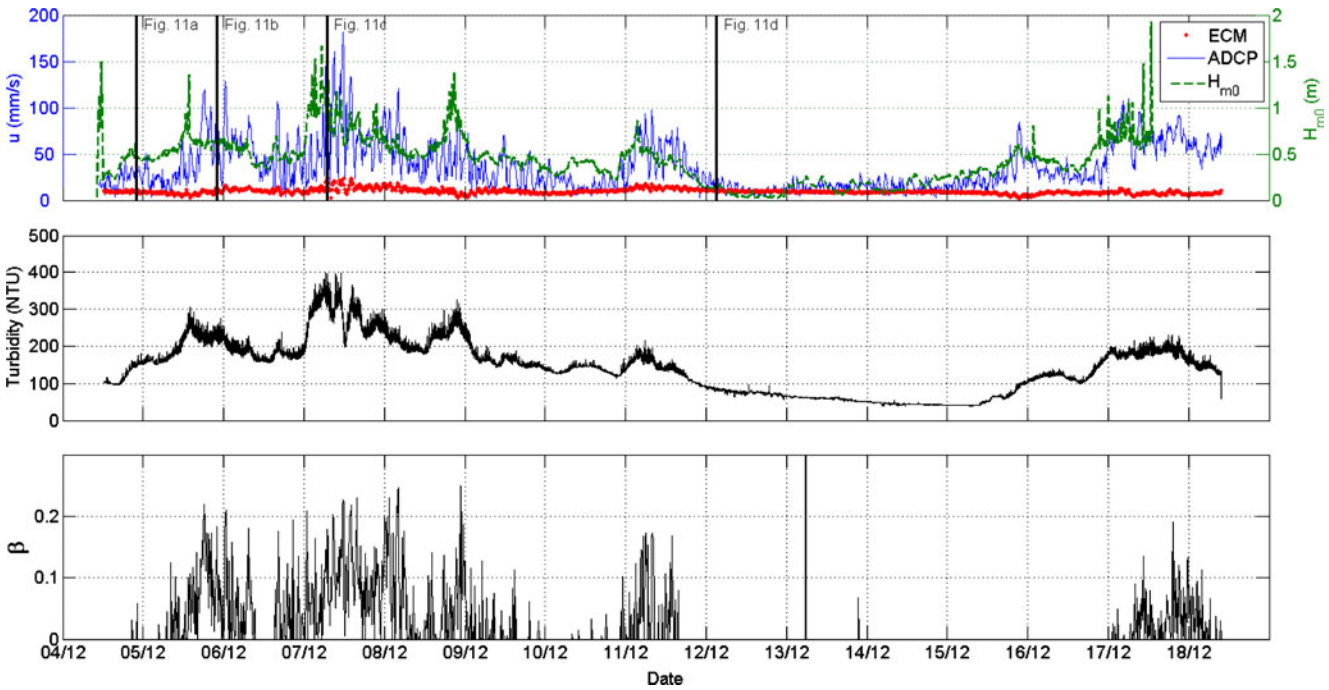

Fig. 8 Time series of flow velocity measured with ADCP and ECM together with wave height (upper diagram) at tower FL42. Middle diagram shows a time series of the turbidity measured about 0.5 m above the bed at the ASM location. The turbidity follows the same pattern as the wave height and flow velocity. Lower diagram shows the time series of the Rouse number (β) computed from the measured concentration profiles by the ASM (Fig. 11). Larger β values are found when waves and flow velocities are large

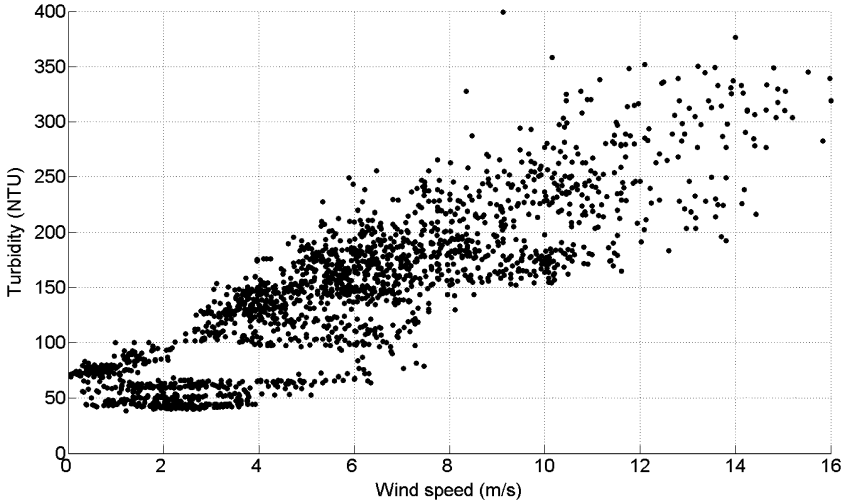

Fig. 9 Scatter plot of turbidity and wind speed; the wind data correspond to those in Fig. 5. Turbidity levels increase more or less linearly with wind speed, hence wave height, e.g., Fig. 5a

hours; and December 12, 0310 hours. Note that the scatter in the profiles is most likely the result of a limited calibration of the ASM sensors (as mentioned, six sensors were calibrated out of 100 in total). Figure 11a shows the sediment concentration profile in the lower 1 m of the water column, just before a storm (H_{m0}=0.45 m, wind speed 6.4 m/s). The concentration is uniformly distributed and has an average value of about 84 mg/l. On December 5, 2200 hours (Fig. 11b), the wind speed increased (H_{m0}=0.66 m, wind speed 10.5 m/s), and a nonuniform concentration profile was measured with large gradients near the bed. On December 7, a storm passed the lake with wind speeds of up to 16 m/s. During this period, large amounts of sediment were suspended in the water column. Figure 11c shows sediment concentration just after the peak of the storm (H_{m0}=0.83 m, wind speed 10.9 m/s). A pronounced nonuniform profile is observed with steep concentration gradients near the bed, where the concentration increased to about 750 mg/l. From other observations, we conclude that in Lake Markermeer such profiles occur when wave height exceeds about 0.5 m (corresponding to a wind speed of about 8 m/s).

When the wind speed further decreased, the concentration dropped and the profile became uniform once again; concentrations of 50 to 100 mg/l occurred. At even smaller wind velocities, i.e., a few meters per second, the fine sediment settled and the concentration dropped to 20–40 mg/l (Fig. 11d, wind speed 1.3 m/s). This erosion, resuspension, and deposition cycle was observed during all storm periods.

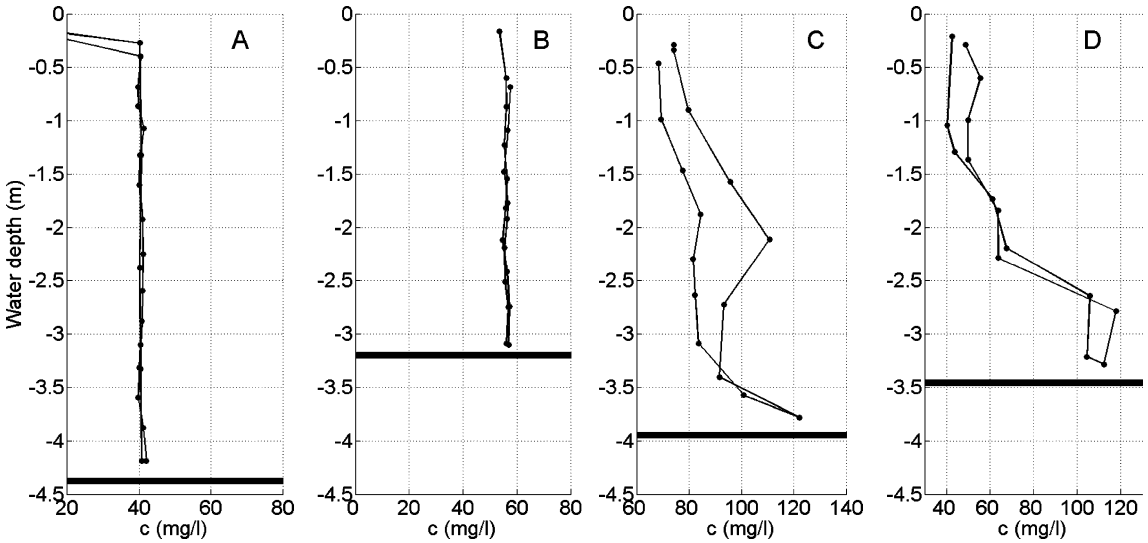

Fig. 10 Sediment concentration measurements with OBS. **a** (November 22, 2007, loc. 11) and **b** (November 26, 2007, loc. 8) show a uniform concentration profile over the vertical, whereas **c** (November 26, 2007, loc. 19) and **d** (November 27, 2007, loc. 15) show a pronounced nonuniform profile

Note that a few sensors measured excessively high concentrations, as a result of which SPM concentrations higher in the water column seem larger than near the bed. This anomaly does not affect our further analysis, and we therefore do not elaborate on this issue.

For all ASM profiles, Rouse profiles were fitted based on the least-squares method, using the Rouse number β (i.e. the slope of the profiles) as the fitting parameter (Winterwerp and van Kesteren 2004),

$$c(z) = c_a \left[\frac{a/h(1-z/h)}{z/h(1-a/h)}\right]^{\beta} \quad \text{with} \quad \beta = \frac{\sigma_T w_s}{\kappa u_*} \tag{1}$$

where c_a is a reference concentration at level a (taken at 0.20 m above the bed), h is the water depth (about 4 m), w_s is the settling velocity (m/s), σ_T the Prandtl–Schmidt number (0.7), κ the Von Karman coefficient (0.4), and u_* the shear velocity. The dotted lines in Fig. 11 show how well these fits match the data; maximum values for β are in the order of 0.25, which is very high for fine grained sediments, and reflect the large vertical gradients, as discussed in the next section.

5 Analysis and discussion

The observations on bed samples reveal a soft, thin oxidized fluffy sediment layer and more solid, but still soft, reduced sediment layer.

We theorize that the fluffy layer is easily mobilized, yielding a more or less homogeneous SPM profile. Most likely, the water column contains an even finer fraction, which only settles after long periods of extremely calm weather, as reflected by a low background concentration in the lake.

During storm, coarse sediment from the soft layer is mobilized. As turbulence is too weak to result in mixing over the entire water column, a near-bed gradient in SPM is generated, as reflected by the large β values in Fig. 11. Hence, modeling fine sediments in the lake requires at least two sediment fractions, a fine fraction and a coarser one.

The sediment fractions are characterized by their settling velocity. The settling velocity, w_s, can be determined from Eq. 1, when values of β and u_* are known. Figure 8c shows a time series of the Rouse number β, computed for every ASM profile during the measurement period.

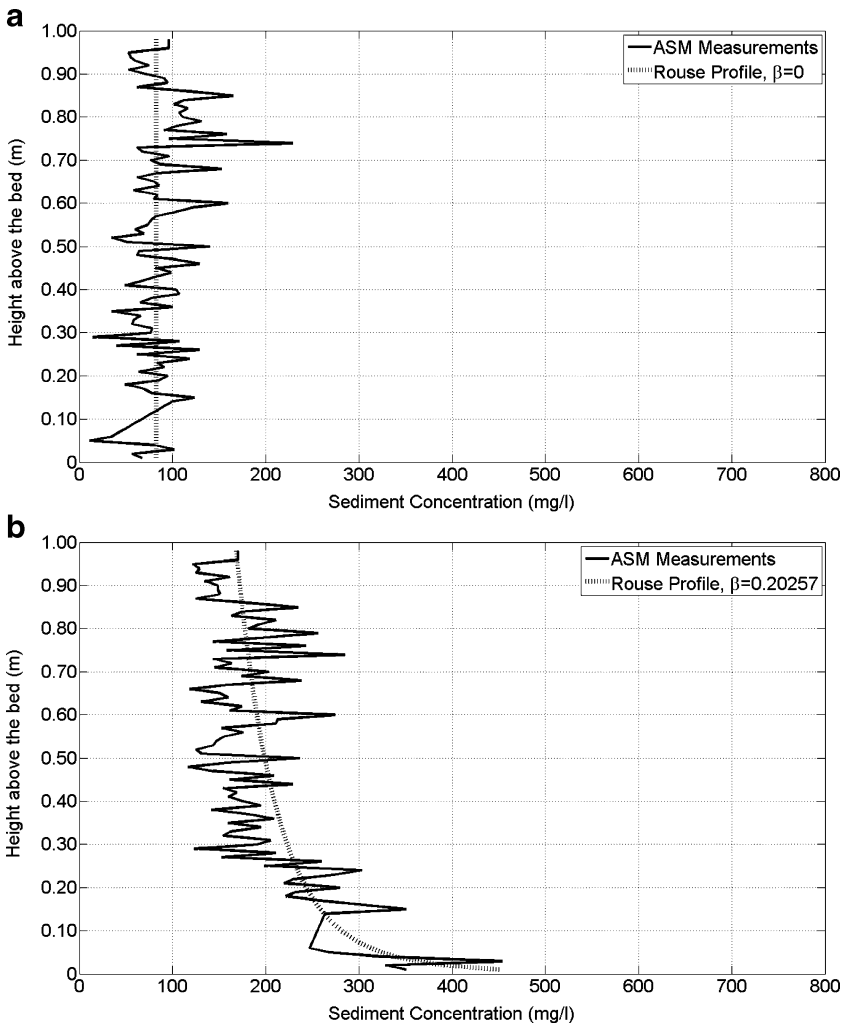

Fig. 11 **a** ASM measurement on Dec. 4, 2007, 2200 hours. **b** ASM measurement on December 5, 2007, 2200 hours. **c** ASM measurement on December 7, 2007, 0650 hours. **d** ASM measurement on December 12, 2007, 0310 hours

Fig. 11 (continued)

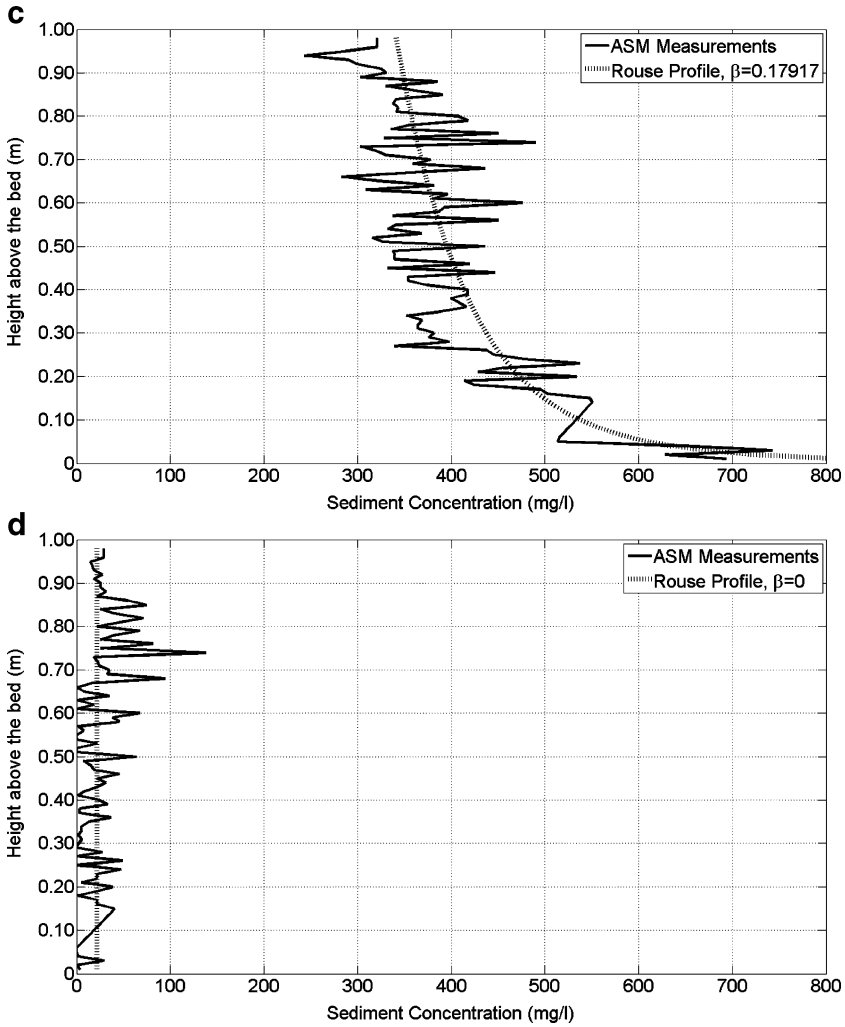

The value of u_* can be determined from the approach of Grant and Madsen (1979), using data from the ADCP and wave heights for the same period (Fig. 8a),

$$u_{*f} = \overline{u}\frac{\sqrt{g}}{C}, \quad u_{*w} = \sqrt{\frac{1}{4}f_w\hat{u}_{orb}^2} \quad \text{and} \quad \left|u_{*fw}\right| = u_* = \sqrt{u_{*f}^2 + u_{*w}^2} \tag{2}$$

where $\overline{u}$ is the depth average current velocity (m/s), C is the Chézy roughness coefficient (set at 60 $m^{1/2}/s$), and the near-bed horizontal orbital velocity amplitude $\hat{u}_{orb}$ (m/s) determined from H_{rms} by the linear wave theory. Subscripts f and w denote flow and waves, respectively. The friction coefficient f_w is determined for hydraulically smooth beds by Whitehouse et al. (2000),

$$f_w = 0.0251\mathrm{Re}_w^{-0.187} \tag{3}$$

where Re_w is the wave Reynolds number, $\mathrm{Re}_w \equiv \hat{u}_{orb}A/\nu$, $A \equiv \hat{u}_{orb}/\omega$, ν is the kinematic viscosity (10^{-6} m^2/s) and $\omega = 2\pi/T$, where T is the wave period. β values are found in the order of 0–0.25 (Fig. 8c). Low values on the order of 0–0.05 represent the fine sediment fraction, and higher values (~0.1–0.25), the coarse fraction.

For several β values, the wave height (H_{m0}) and depth average velocity ($\overline{u}$) are estimated from Fig. 8a. The wave period (T) was not measured in this campaign and is therefore estimated from earlier studies (Van Ledden et al. 2006).

This analysis results in representative values of the settling velocities for both fractions (Table 2). The settling velocity for the fine fraction is limited to a maximum of 0.1 mm/s, whereas the coarser fraction shows settling velocities on the order of 0.5 to 4 mm/s. Earlier measurements (Table 1) show much lower settling velocities of the same order as the settling velocity for the fine fraction in Table 2. As the settling velocities in Table 1 are determined from sediment samples partly taken from sediment traps placed higher in the water column, this is expected. The ASM measurements near the bed thus also show that coarser sediment can be suspended in the water column as well and generate steep concentration gradients near the bed.

To examine sediment dynamics for the full range of conditions and over the entire water column, a 1DV point model (Winterwerp 2001; Winterwerp and van Kesteren 2004) was used. With these model simulations, the conceptual picture of the sediment dynamics is verified. Mud dynamics in Lake Markermeer is described by means of a two-fraction representation of the grain size distribution of mud; a fine fraction (w_s=0.025 mm/s) and a coarse (w_s=0.8 mm/s) fraction. Model settings, such as settling velocities, initial concentrations, and hydrodynamic forcing, are based on calibration results of a large Delft3D model of the lake (Vijverberg 2008). These settling velocity values show good agreement with the computed values from the ASM measurements (Table 2). However, the coarsest sediment fraction is not included in the 1DV model. Further, model development should include an additional, coarser sediment fraction to better describe sediment dynamics during extreme conditions. For the sake of simplicity, the present analysis is carried out with two sediment fractions.

Results of the 1DV model simulations are shown in Fig. 12. The observed cycles of erosion and deposition of the both sediment fractions can be described as follows.

During very low wind speeds (1 to 2 m/s), both fractions can settle from the water column forming a thin, high-concentration layer near the bed. If wind speed increases to about 4 m/s, the fine fraction is resuspended rapidly and is almost uniformly distributed over the vertical (Fig. 12a). If the wind speed further increases, the fine fraction becomes uniformly mixed with a concentration of about 80 mg/l (Fig. 12b).

In this situation, the coarse fraction remains on the bed. Even if the wind speed increases to about 8 m/s, this high-concentration layer remains on the bed (Fig. 12c). Only if the wind speed increases further (10 m/s or more) does the coarse fraction get resuspended. At the onset of the storm, this high-concentration layer continues to be near the bed (Fig. 12d, wind speed 15 m/s). At the peak of storm (flow velocity increased to 0.20 m/s), the coarse fraction is almost uniformly mixed (Fig. 12e), resulting in a concentration of about 150–200 mg/l (with total sediment concentration of about 200–300 mg/l). After the peak of storm, the wind speed decreases and the coarse fraction settles first, thus forming the high-concentration layer near the bed with concentrations of up to about 1 g/l (Fig. 12d). If a series of consecutive storms were to occur, a high-concentration layer would not form and the sediment would remain in suspension. For wind speeds below 2 m/s, the fine fraction also settles. It can be concluded that the high-concentration layer near the bed, containing the coarse fraction, only occurs at the onset and towards the end of a storm period, when wind speeds change rapidly. During the peak of storm, the high-concentration near-bed layer is absent.

Table 2 Results of the settling velocity analysis: representative values for the settling velocity, computed from the wave height, wave period, depth average flow velocity, and Rouse number β

Fraction	β	H_{m0} (m)	T (s)	u (m/s)	w_s (mm/s)
Fine	0.05	0.3	2.3	0.03	0.090
Coarse	0.1	0.5	3.0	0.07	0.5
	0.2	1.0	4.0	0.15	2.3
	0.25	1.2	4.5	0.20	3.7

As also shown in Fig. 12, the high-concentration layer influences the eddy diffusivity and the flow velocity profile near the bed. When this layer is present, the eddy diffusivity decreases drastically inside this layer, as well as the flow velocity (Fig. 12c and d). Turbulence is damped, resulting in less mixing capacity, which stabilizes the layer. This sediment–fluid interaction has been observed in many aquatic bodies. To our knowledge, such interactions have not been reported before in low-dynamics systems. Yet, we infer that they do occur in shallow lakes, if fine sediment is abundant on the bed.

In summary, the model results explain the pronounced vertical structure of suspended sediment in the lake. This nonuniformity has not been recognized before in Lake Markermeer.

6 Implication for design of hydraulic works

Numerical models are often used to design and assess the effectiveness of measures to reduce turbidity. Based on the findings of this work, it is concluded that the design of various mitigation measures, such as deep pits, benefits from the use of 3D models, instead of 2D. Deep pits can act as traps for fine sediments, which are thus isolated from the system and no longer affect light penetration. This results in lower sediment concentrations in the water column in proximity to the trap. The vertical structure in the sediment concentration outside the trap, together with high-concentration layers near the bed, increase the mixture density near the bed. At the edge of the trap, a horizontal density gradient occurs. As a result, density currents can be generated near the trap, inducing sediment transport into the trap. This may well be associated with large quantities of sediment into the pit (or navigation channel) as can be seen from the following order of magnitude assessment:

The flow velocity induced by density currents is estimated (Kranenburg 1998) at

$$\overline{u_{dc}} = \frac{1}{2}\sqrt{\Delta\rho g d} \tag{4}$$

where d is the thickness of the high-concentration layer (m) and $\Delta\rho$ the horizontal density difference between the

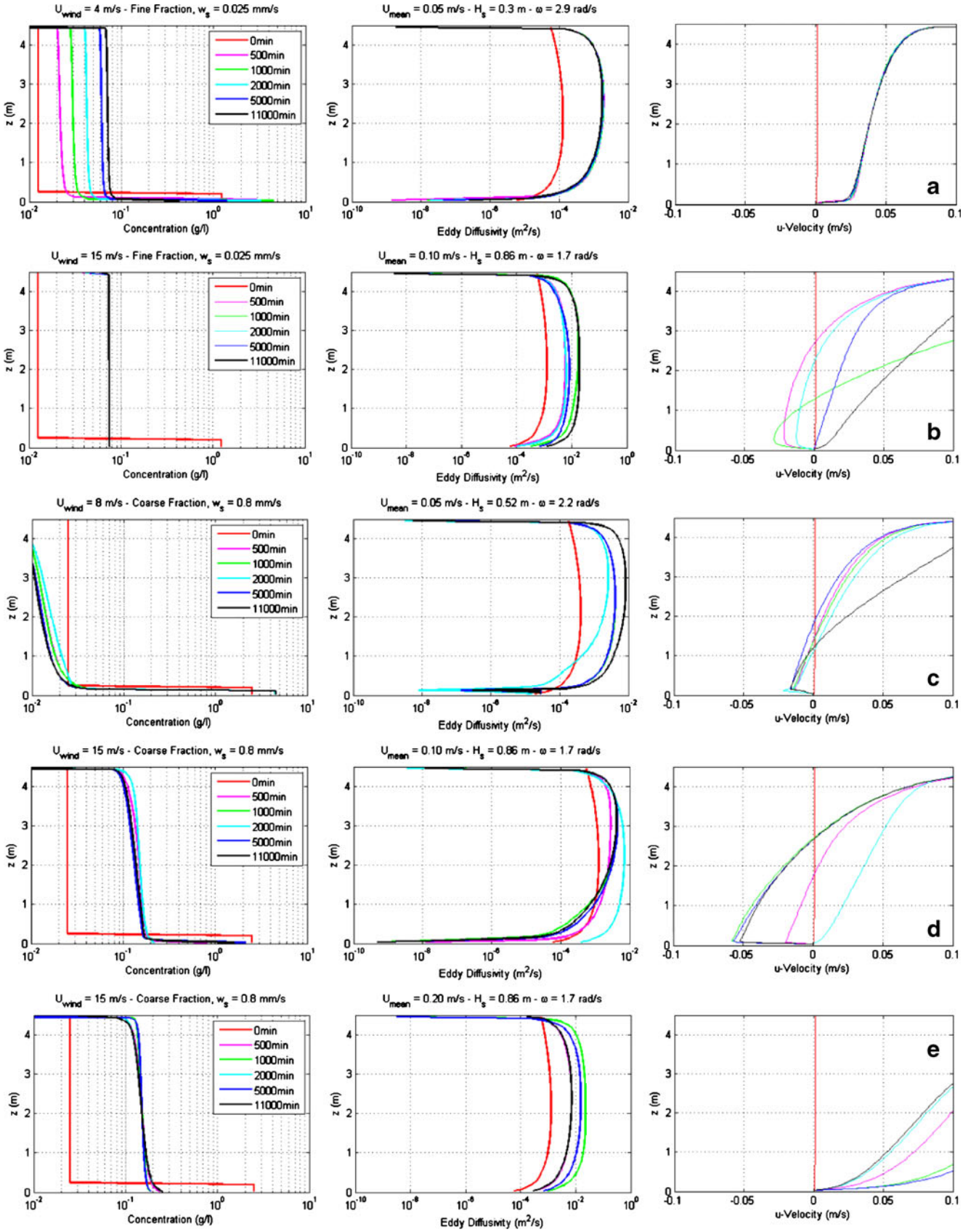

Fig. 12 1DV model results—behavior of fine and coarse mud fractions for several wind conditions

suspension inside and outside the trap (kg/m^3). The relation between the density and sediment concentration is given by the equation of state (Winterwerp and van Kesteren 2004),

$$\rho\left(S,\theta,c^{(i)}\right)=\rho_w(S,\theta)+\sum_i\left\{\left(1-\frac{\rho_w(S,\theta)}{\rho_s^{(i)}}\right)c^{(i)}\right\} \tag{5}$$

where ρ_w is the density (kg/m^3) of water as a function of the temperature (θ) and salinity (S), ρ_s is the solid density (kg/m^3) of the mud fraction i and c is the concentration of the fraction (kg/m^3). A typical value for the concentration differences in Lake Markermeer is 1 kg/m^3, and the layer thickness is about 0.10 m. For these values u_{dc} is approximately 0.02 m/s, which is 10–20% of the wind-induced flow velocities of 0.1 to 0.2 m/s.

The sediment flux due to density currents is then estimated at

$$\mathrm{Flux_{dc}}=0.02(\mathrm{m/s})\times 1\,\mathrm{kg/\,m^3}\times 0.1\,\mathrm{m}=0.002\mathrm{kg/s/m}$$

The flux into a rectangular trap with length L and width B is 0.002 ($2L+2B$; kg/s). The density current is always directed towards the trap.

The sediment flux due to wind induced flow is, typically:

$$\begin{aligned}\mathrm{Flux_{ad}}&=0.1\mathrm{m/s}\times 0.05\mathrm{kg/m^3}\times 3.6\mathrm{m(mean\ water\ depth)}\\&=0.018\mathrm{kg/s/m}.\end{aligned}$$

We define the trapping efficiency E of a rectangular trap with length L as,

$$E=\frac{w_s}{h}\frac{L}{U} \tag{6}$$

where w_s is the settling velocity, h the water depth (set at 3.6 m), and U the depth average flow velocity (set at 0.1 m/s).

For the fine fraction (w_s= 0.025 mm/s), $E=0.07\times 10^{-3}L$. For the coarse fraction (w_s= 0.8 mm/s), E is computed as $E=2.2\times 10^{-3}L$.

The flux into the trap is now computed as $E\mathrm{Flux_{ad}}B$. The factor B is the width of the trap. This results in a range between $1.25\times10^{-6}LB$ (kg/s) and $40\times10^{-6}LB$ (kg/s). A typical dimension of a trap in Lake Markermeer is 400×400 m (Van den Brenk 2002). The flux due to density current is in that case 3.2 kg/s, the flux due to advection 0.2–6.4 kg/s. For smaller traps (e.g., 100×100 m), the density current-induced flux will be larger than the flux due to advection. For longer traps (L larger than B), the advection-induced infill flux becomes increasingly important relative to the density-induced flux.

The above analysis is a rough estimation procedure and therefore has the following limitations:

- The assessment of the trap efficiency E is based on still water conditions. In flowing water, vertical mixing occurs, reducing the net deposition of fines towards the bed and/or into the pit. A local depression in the lake bed attracts flow, as shown in model simulations (Vijverberg 2008). As a result, the current velocities may even increase if the pit is large enough. Moreover, the scale of the larger eddies increases beyond the undisturbed water depth. Therefore, E can be expected to be at least an order of magnitude smaller. Advective fluxes will then be reduced to order 0.02–0.6 kg/s. However, the actual value of E can only be obtained from detailed 3D modeling.
- Density currents only occur during certain times (e.g., during the onset and towards the end of a storm). The advective flux is always present. This analysis only gives fluxes, so it does not address these differences.

The above estimation shows that the density current flux can be at least in the same order as the advective flux. This indicates that density currents can significantly contribute to the accumulation of sediments in the trap. Large accumulation rates were also observed in the lake from a few bottom surveys in historical deep pits (Van den Brenk 2002). Accumulation rates were found to be much larger than expected from settling of sediment only. This suggests as well that density currents in the lake play an important role (Vijverberg 2008). Consequently, the effectiveness of mitigation measures is affected by these processes.

7 Conclusions

Results of this study enhanced our understanding of fine sediment dynamics in Lake Markermeer. Layers with high sediment concentration near the bed were measured during some stormy conditions. Model simulations confirm that such layers can occur. These findings support our hypothesis that sediment dynamics in the lake is characterized by pronounced 3D structures. This insight has consequences for field measurements and modeling studies of the Lake and for the design and analysis of mitigation measures for turbidity. Further field measurements should focus on measurements over the total height of the water column, with more detailed measurements near the bed. Numerical modeling studies will benefit from the use of fully 3D models inclusive of density effects and sediment–fluid interaction in order to account for these processes.

References

Cundy AB, Lafite R, Taylor JA, Hopkinson L, Deloffre J, Charman R, Gilpin M, Spencer KL, Carey PJ, Heppell CM, Ouddane B, de Wever S, Tuckett A (2007) Sediment transfer and accumulation in two contrasting salt marsh/mudflat systems: the Seine estuary (France) and Medway estuary (UK). Hydrobiologia 588:125–134

Facchinelli A, Gallini L, Barberis E, Magnoni M, Hursthousem AS (2001) The influence of clay mineralogy on the mobility of radiocesium in upland soils of northwest Italy. J Environ Radioactiv 56:299–307

Grant WD, Madsen OS (1979) Combined wave and current interaction with a rough bottom. J Geophys Res 84(C4):1797–1808

Jin KR, Ji Z-G (2004) Case study: modeling of sediment transport and wind-wave impact in Lake Okeechobee. J Hydraul Eng 130(11):114–125

Jin KR, Sun D (2007) Sediment resuspension and hydrodynamics in Lake Okeechobee during late summer. J Eng Mech 133(8):899–910

Kranenburg C (1998) Density currents CT5302. Delft University of Technology, Lecture note

Lenselink G, Menke U (1995) Geologische en bodemkundige atlas van het Markermeer (in Dutch). Rijkswaterstaat, Directie IJsselmeergebied, Lelystad. ISBN 90-369-1148-6

McAnally WH, Teeter A, Schoellhamer D, Friedrichs C, Hamilton D, Hayter E, Shrestha P, Rodriguez H, Sheremet A, Kirby R (2007) Management of fluid mud in estuaries, bays and lakes II: measurement, modelling and management. J Hydraul Eng 133:23–38

Sanada Y, Matsunagaa T, Yanasea N, Nagaoa S, Amanoa H, Takadab H, Tkachenko Y (2002) Accumulation and potential dissolution of Chernobyl-derived radionuclides in river bottom sediment. Appl Radiat Isot 56:751–760

van den Brenk, S (2002). Sedimentatieonderzoek vaargeulen (in Dutch). Rijkswaterstaat, Directie IJsselmeergebied, December 2002.

van Duin, EHS (1992) Sediment transport, light and algal growth in the Markermeer—a two dimensional water quality for a shallow lake. Ph.D. thesis, Wageningen University.

van Duin EHS, Blom G, Lijklema L, Scholten MJM (1992) Aspects of modelling sediment transport and light conditions in Lake Marken. Hydrobiologia 235(236):167–176

van Kessel, T., Boer, G. de, Boderie, P. (2008). Calibration suspended sediment model Markermeer. Deltares, report Q4612

van Ledden, M., Gerrits, G., van Kessel, T., Mosselman, E. (2006). Verdiepingsslag en maatregelen slibproblematiek Markermeer—analyse kennisleemten en inventarisatie maatregelen (in Dutch). Royal Haskoning, report 9R3456.A0.

van Wijngaarden M, Venema LB, de Meijer RJ (2002) Radiometric sand-mud characterisation in the Rhine-Meuse estuary—Part A Fingerprinting. Geomorphology 43:87–101

Vijverberg, T. (2008). Mud dynamics in the Markermeer—silt traps as a mitigation measure for turbidity. MSc. Thesis, Delft University of Technology.

Vlag DP (1992) A model for predicting waves and suspended silt concentration in a shallow lake. Hydrobiologia 235(236):119–131

Whitehouse R, Soulsby R, Roberts W, Mitchener H (2000) Dynamics of estuarine muds. HR Wallingford DETR Thomas Telford, London, p 210

Winkels, H.J. (1997). Contaminant variability in a sedimentation area of the river Rhine. Ph. D. thesis, Wageningen University.

Winterwerp JC (2001) Stratification effects by cohesive and non-cohesive sediment. J Geophys Res 106(C10):22559–22574

Winterwerp, J.C., and Van Kesteren, W.G.M. (2004). Introduction to the physics of cohesive sediments in the marine environment. 1st edition. Elsevier